GROWTH OF THE ZETA FUNCTION FOR A QUADRATIC MAP AND THE DIMENSION OF THE JULIA SET

JOHN STRAIN AND MACIEJ ZWORSKI

1. Introduction

In this note we present theoretical upper bounds and numerical lower bounds for the number of zeros of the Ruelle zeta function associated to a quadratic map with a real Cantor-like Julia set.

By adapting the methods of [9], which become easier for such maps, we show that for s in strips parallel to the imaginary axis, the zeta function is bounded by $\exp(C|s|^{\delta})$ where δ is the dimension of the Julia set. The proof of this upper bound suggests a fast algorithm for computing the number of zeros. The numerical results computed with this algorithm indicate that the upper bound is optimal and that the density of zeros in strips is related to the dimension of the Julia set.

Our motivation comes from the study of the distribution of quantum resonances — see [23] for a general introduction and [9, 13] for discussions of the specific bounds considered here. The relation between the density of resonances and the fractal dimensions of classical trapped sets was first studied by Sjöstrand [20] for quantum resonances associated to Schrödinger operators, $-h^2\Delta+V(x)$ for which the classical flow, associated to the Hamiltonian $\xi^2+V(x)$, was hyperbolic. A typical example is the three-bump potential shown in Fig. 1. After we define the relevant objects for $z \mapsto z^2 + c$ we will present the analogy to this setting in Table 1.

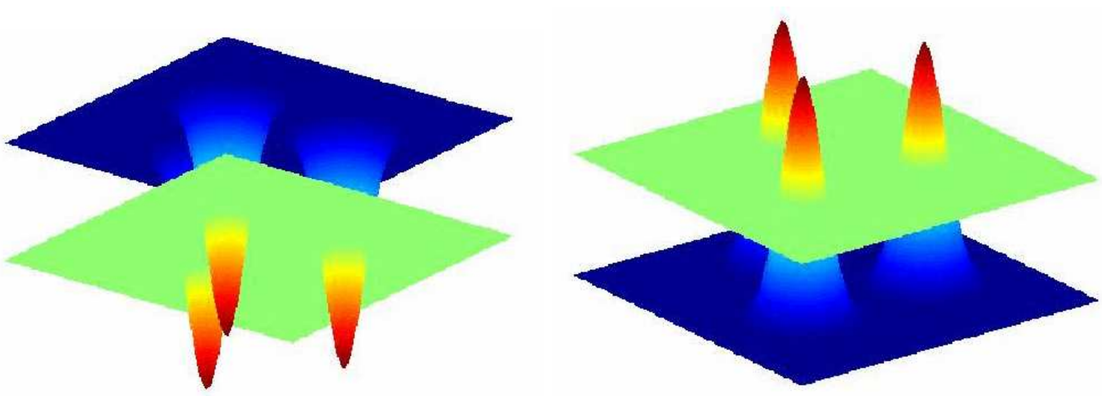

Figure 1. A three-well confining potential and a three-bump potential with the energy at which the flow is hyperbolic. The density of resonances for the latter was studied numerically in [11], [12].

Motivated by [9], where the model was a Schottky quotient, we can consider the dynamical system associated to

$$f_c(z) = z^2 + c\,, \quad c < -2\,, \tag{1.1}$$

as the simplest model for the relation between scattering resonances and chaotic dynamics: the zeros of the dynamical zeta function provide a convenient model for quantum resonances. It would be interesting to see if they do coincide with suitably defined resonances of *hyperbolic laminations* [14].

TABLE 1. Analogies between the Schrödinger operator [20], convex co-compact hyperbolic quotient [9],[18],[22] and $z \mapsto z^2 + c$ settings [4].

$P(h) = -h^2\Delta + V(x)$	$X = \Gamma\backslash\mathbb{H}^n$	$z \mapsto z^2 + c$
quantum resonances, z, of $P(h)$, $\mathrm{Re}\, z \sim E$, $\mathrm{Im}\, z > -Ch$	quantum resonances, $s(n-1-s)$, $\lvert\mathrm{Im}\, s\rvert \sim 1/h$ and $\mathrm{Re}\, s > -C$ of $-\Delta_X$	**?**
?	zeros of the zeta function $Z_\Gamma(s)$ coinciding with the quantum resonances of Δ_X	zeros of $Z(s)$ with $\lvert\mathrm{Im}\, s\rvert \sim 1/h$ and $\mathrm{Re}\, s > -C$
Trapped set at energy E on a Poincaré section	Limit set of Γ, $\Lambda(\Gamma)$	Julia set, $J(c)$
Dimension, m, of the trapped set for energies near E	$m = 2(\delta+1)$, $\delta = \dim(\Lambda(\Gamma))$	$m = 2(\delta+1)$, $\delta = \dim(J(c))$

The Ruelle zeta function is defined in terms of the Ruelle transfer operator

$$\mathcal{L}(s)u(z) = \sum_{f_c(w)=z} [f_c'(w)]^{-s} u(w)\,, \tag{1.2}$$

where $[f_c'(w)]$ is the holomorphic continuation of $|f_c'(w)|$ defined on the real axis and z^{-s} is the principal branch of the usual complex power function. On an appropriately chosen space of functions, $\mathcal{L}(s)$ is a trace class operator so the Ruelle zeta function can be defined by

$$Z(s) = \det(I - \mathcal{L}(s))\,. \tag{1.3}$$

An equivalent purely dynamical product representation, which converges for $\mathrm{Re}\, s \gg 1$, is given by [10]

$$Z(s) = \exp\left(-\sum_{n=1}^{\infty} \frac{1}{n} \sum_{f^{\{n\}}(z)=z} \frac{[(f^{\{n\}})'(z)]^{-s}}{1 - [(f^{\{n\}})'(z)]^{-1}} \right)\,. \tag{1.4}$$

Here we have dropped the parameter c from the notation and denoted by $f^{\{n\}} = f \circ f^{\{n-1\}}$, $f^{\{0\}} = \mathrm{id}$, the n-fold composition of f with itself. We prove the following asymptotic upper bound for Z in terms of the dimension δ of the Julia set

$$J = \overline{\bigcup_{n\geq 1} \{z \ : \ f^{\{n\}}(z) = z\}} \tag{1.5}$$

of f:

Theorem 1. *Let f be the quadratic map defined by* (1.1)*, let δ be the dimension of the Julia set J defined by* (1.5)*, and let Z be the dynamical zeta function defined by* (1.4)*. Then for any C_0, there exists C_1 such that*

$$|Z(s)| \leq C_1 \exp(C_1 |s|^\delta) \tag{1.6}$$

for $|\mathrm{Re}\, s| \leq C_0$.

The proof of this result is quite simple; we design our spaces carefully and analyze the determinant of the Ruelle transfer operator by L^2-techniques. As in [9], more complicated Cantor set repellers can be treated by a self-similarity argument based on the Koebe Distortion Lemma in place of the cookie-cutter arguments used in Section 3 below. However, for simplicity of exposition we consider only the case $z \mapsto z^2 + c$. The case of general hyperbolic rational function was recently proved by Christiansen [4].

Since the product representation (1.4) of the zeta function converges for $\mathrm{Re}\, s$ large, Jensen's theorem yields

Corollary 2. *Let $m(s)$ be the multiplicity of the zero of Z at s and*

$$n(r, x) = \sum \{m(s) \ : \ |\mathrm{Im}\, s| \leq r\,, \quad \mathrm{Re}\, s > x\}. \tag{1.7}$$

Then for any real x,

$$n(r+1, x) - n(r, x) = \sum \{m(s) \ : \ r \leq |\mathrm{Im}\, s| \leq r+1\,, \quad \mathrm{Re}\, s > x\} \leq C_1 r^\delta, \tag{1.8}$$

where $\delta = \dim J$. By summation,

$$n(r, x) \leq C_2 r^{1+\delta}. \tag{1.9}$$

As far as lower bounds are concerned we present the following

Conjecture 3. *The bound* (1.9) *is optimal, in the sense that for $x > x_0$, with some fixed $x_0 = x_0(c)$,*

$$n(r, x) \geq C_3(x) r^{1+\delta}$$

for sufficiently large r.

As we will describe in Section 6 below this conjecture is strongly supported by the numerical evidence. These numerical results provide further evidence for the existence of *fractal Weyl laws* in situations with chaotic classical dynamics.

In view of the lack of rigorous examples for quantum resonances, it would be very interesting to know whether this upper bound is optimal. When the Julia set is not a Cantor set the upper bound may not be optimal, as in the simple example $f(z) = z^2$ where $J(f) = \{z \ : \ |z| = 1\}$ and $Z(s) = 1 - 2^{s-1}$.

2. The transfer operator on L^2 spaces

To connect the two definitions (1.3) and (1.4) of the zeta function, we modify the discussion in [10]. Construct a neighborhood D of the Julia set J by

$$\begin{gathered} D = D_1 \cup D_2, \quad D_j \text{ open neighbourhoods of } J \cap (-1)^j(0,\infty) \\ \overline{g_i(D_j)} \subset D_i\,, \quad f \circ g_i(z) = z\,. \end{gathered} \tag{2.1}$$

More explicitly, $g_i(z) = (-1)^i\sqrt{z-c}$ with a branch of the square root chosen to be positive on the positive real axis. The D_j's can be neighbourhoods of $(-1)^j[\sqrt{-c-\xi_c}, \xi_c]$, where

$$\xi_c = (1+\sqrt{1/4-c})/2$$

is the largest fixed point of f_c.

The Ruelle transfer operator (1.2) then becomes

$$\mathcal{L}(s)u(z) = \sum_{i=1}^{2}[g_i'(z)]^s u(g_i(z))\,, \quad z \in D_j \tag{2.2}$$

acting on functions u in

$$H^2(D) = \{u \text{ holomorphic in } D \;\;:\;\; \iint_D |u(z)|^2 dm(z) < \infty\}\,.$$

The only difference from (1.2) and [10] lies in choosing L^2 spaces of holomorphic functions instead of Banach spaces. However, we can still prove the analogue of (a special case of) a result of Ruelle [19] and Fried [7]:

Proposition 1. *Suppose that the Ruelle operator $\mathcal{L}(s) : H^2(D) \to H^2(D)$ is defined by* (2.2) *and $c < -2$. Then for all $s \in \mathbb{C}$, the operator $\mathcal{L}(s)$ is trace-class and*

$$|\det(I - \mathcal{L}(s))| \leq \exp(C|s|^2)\,. \tag{2.3}$$

Proof. The proof is based on estimates of the singular values $\mu_l(\mathcal{L}(s))$. We will show that there exists $C > 0$ such that

$$\mu_l(\mathcal{L}(s)) \leq e^{C|s| - l/C}\,. \tag{2.4}$$

First we recall some basic properties of singular values of a compact operator $A : H_1 \to H_2$ where H_j's are Hilbert spaces. We define

$$\|A\| = \mu_0(A) \geq \mu_1(A) \geq \cdots \geq \mu_\ell(A) \to 0\,,$$

to be the eigenvalues of $(A^*A)^{\frac{1}{2}} : H_1 \to H_1$, or equivalently of $(AA^*)^{\frac{1}{2}} : H_2 \to H_2$. The min-max principle shows that

$$\mu_\ell(A) = \min_{\substack{V \subset H_1 \\ \operatorname{codim} V = \ell}} \max_{\substack{v \in V \\ \|v\|_{H_1} = 1}} \|Av\|_{H_2}\,. \tag{2.5}$$

The following rough estimate suffices: suppose that $\{\rho_j\}_{j=0}^\infty$ is an orthonormal basis of H_1. Then

$$\mu_\ell(A) \leq \sum_{j=\ell}^{\infty} \|A\rho_j\|_{H_2}\,. \tag{2.6}$$

Indeed, for $v \in V_\ell = \text{span}\,\{\rho_j\}_{j=\ell}^\infty$ in (2.5), the Cauchy-Schwartz inequality and the usual $\ell^2 \subset \ell^1$ inequality yield

$$\|Av\|_{H_2}^2 = \left\| \sum_{j=\ell}^\infty \langle v, \rho_j \rangle_{H_1} A\rho_j \right\| \leq \|v\|_{H_1}^2 \left(\sum_{j=\ell}^\infty \|A\rho_j\|_{H_2} \right)^2 ,$$

from which (2.5) gives (2.6).

We will also need some more sophisticated results about singular values. The first is the *Weyl inequality* [8]: if $H_1 = H_2$ and $\lambda_j(A)$ are the eigenvalues of A, then

$$|\lambda_0(A)| \geq |\lambda_1(A)| \geq \cdots \geq |\lambda_\ell(A)| \to 0 \,,$$

then for any $N \geq 0$,

$$\prod_{\ell=0}^N (1 + |\lambda_\ell(A)|) \leq \prod_{\ell=0}^N (1 + |\mu_\ell(A)|) \,.$$

In particular, if the operator A is trace-class so $\sum_\ell \mu_\ell(A) < \infty$, then the definition

$$\det(I + A) \ := \prod_{\ell=0}^\infty (1 + \lambda_\ell(A))$$

makes sense and

$$|\det(I + A)| \leq \prod_{\ell=0}^\infty (1 + \mu_\ell(A)) \,. \tag{2.7}$$

We will also require the following standard inequality about singular values [8]:

$$\mu_{\ell_1+\ell_2}(A + B) \leq \mu_{\ell_1}(A) + \mu_{\ell_2}(B) \tag{2.8}$$

We finish the review, as we started, with an obvious equality: suppose that $A_j : H_{1j} \to H_{2j}$ and we form $\bigoplus_{j=1}^J A_j : \bigoplus_{j=1}^J H_{1j} \to \bigoplus_{j=1}^J H_{2j}$, as usual, $\bigoplus_{j=1}^J A_j(v_1 \oplus \cdots \oplus v_J) = A_1 v_1 \oplus \cdots \oplus A_J v_J$. Then

$$\sum_{\ell=0}^\infty \mu_\ell \left(\bigoplus_{j=1}^J A_j \right) = \sum_{j=1}^J \sum_{\ell=0}^\infty \mu_\ell(A_j) \,. \tag{2.9}$$

With these preliminary facts taken care of, we see that (2.4) implies (2.3). In fact, (2.7) shows that

$$\det(I - \mathcal{L}(s)) \leq \prod_{\ell=0}^\infty (1 + e^{C|s| - \ell/C}) \leq e^{C^3|s|^2} \,.$$

Hence it remains to establish (2.4). For that we choose the D_j's to be symmetric discs containing $(-1)^j[(\xi_c + c)^{1/2}, \xi_c]$ and disjoint from $i\mathbb{R}$. We decompose

$$H^2(D) = \bigoplus_{j=1}^2 H^2(D_j)$$

and define

$$\mathcal{L}_{ij}(s) : H^2(D_i) \to H^2(D_j)$$

by

$$\mathcal{L}_{ij}(s)u(z) := [g_i'(z)]^s u(g_i(z))$$

for $z \in D_j$. The standard inequality (2.8) and a version of (2.9) then yield

$$\mu_\ell(\mathcal{L}(s)) \leq \max_{1\leq i,j\leq 2} 2\mu_{[\ell/4]}(\mathcal{L}_{ij}(s)) .$$

To estimate $\mu_k(\mathcal{L}_{ij}(s))$ we use the rough estimate (2.6), with an orthonormal basis $\{\rho_k\}$ of $H^2(D_i)$ composed of the centered and scaled monomials

$$\rho_k(z) = \frac{\sqrt{2k+1}}{r_i}\left(\frac{z-a_i}{r_i}\right)^k ,$$

where $D_i = D(a_i, r_i)$ has center a_i and radius r_i. Since $\overline{g_i(D_j)} \subset D_j$,

$$\|((g_i(z)-a_i)/r_i)^k\|_{H^2(D_i)} \leq C\alpha^k ,$$

for some $0 < \alpha < 1$. Since $|[g_i(z)]^s| \leq e^{C|s|}$, we obtain

$$\mu_\ell(\mathcal{L}_{ij}(s)) \leq C\sum_{k\geq\ell} \|\mathcal{L}_{ij}(s)(\rho_k)\| \leq C\sum_{k\geq\ell} e^{C|s|}\alpha^k \leq Ce^{C|s|}\frac{\alpha^\ell}{1-\alpha} \leq C_1 e^{C|s|-\ell/C_1} ,$$

for some C_1, which completes the proof of (2.4). □

The next proposition follows by an easy modification of the standard argument (see for instance [10]):

Proposition 2. *Let* $\mathcal{L}(s)$ *be defined by* (1.2). *Defining the determinant as in Proposition 1 we have*

$$\det(I-\mathcal{L}(s)) = \exp\left(-\sum_{n=1}^\infty \frac{1}{n}\sum_{f^{\{n\}}(z)=z} \frac{[(f^{\{n\}})'(z)]^{-s}}{1-[(f^{\{n\}})'(z)]^{-1}}\right) ,$$

for $\operatorname{Re} s \gg 0$. *Hence the left hand side provides an entire analytic continuation of the right hand side.*

Proof. Fix $s \in \mathbb{C}$. Then (2.4) and (2.7) imply that

$$h(\lambda) := \det(I-\lambda\mathcal{L}(s))$$

is an entire function of order 0. For $|\lambda|$ sufficiently small, the power series of $\log(I-\lambda\mathcal{L}(s))$ converges [8] so

$$\det(I-\lambda\mathcal{L}(s)) = \exp(\operatorname{tr}\log(I-\lambda\mathcal{L}(s))) = \exp\left(-\sum_{n=1}^\infty \frac{\lambda^n}{n}\operatorname{tr}(\mathcal{L}(s))^n\right) . \tag{2.10}$$

To analyze the traces, we go back to the first definition (1.2) of the transfer operator:

$$\mathcal{L}(s)u(z) = \sum_{f(w)=z} [f'(w)]^{-s}u(w) .$$

The Schwartz kernel of $\mathcal{L}(s)^n$ can be written in terms of the Bergman kernel for the D_j's, so the evaluation of the trace† gives

$$\operatorname{tr}\mathcal{L}(s)^n = \sum_{f^{\{n\}}(z)=z} \frac{[(f^{\{n\}})'(z)]^{-s}}{1-[(f^{\{n\}})'(z)]^{-1}} .$$

†To see how it works, consider the simple case where f is holomorphic in the unit disc, $f(0)=0$, and $|f(z)|<|z|$ for $z \neq 0$. By Cauchy's formula, pullback by f is an integral operator on $H^2(D(0,1))$ with kernel $\pi^{-1}(1-f(z)\bar{\zeta})^{-2}$. and trace $\pi^{-1}\iint_{D(0,1)}(1-f(z)\bar{z})^{-2}dm(z) = (1-f'(0))^{-1}$. In our case $f'(0)$ is always real and we obtain an absolute value as we move between different discs when $f'(0)<0$.

Returning to (2.10), we obtain for $\operatorname{Re} s$ sufficiently large,

$$\det(I - \lambda \mathcal{L}(s)) = \exp\left(-\sum_{n=1}^{\infty} \frac{\lambda^n}{n} \sum_{f^{\{n\}}(z)=z} \frac{[(f^{\{n\}})'(z)]^{-s}}{1 - [(f^{\{n\}})'(z)]^{-1}} \right) .$$

Setting $\lambda = 1$ and employing (1.4) proves the proposition. □

Note that the proof did not use any properties of the open sets D_j other than the ones given in (2.1).

3. Estimates in terms of the dimension of J.

For the proof of the Theorem 1, we will choose the D_j's in the definition of $\mathcal{L}(s)$ to depend on the size of s. Let $h = 1/|s|$. The self-similar structure of J suggests that $D_j = D_j(h)$ should be a union of $\mathcal{O}(h^{-\delta})$ disjoint discs with radii $r \sim h$, separated from J by $d(\partial D_j, J) \sim h$. The argument used in the proof of Proposition 1 will then give (1.6).

We begin with

Proposition 3. *Let $J \subset \mathbb{R}$ be the Julia set for* (1.1). *Then there exist constants δ_0 and $K = K(c)$ such that for $\delta < \delta_0$, the connected components of $J + [-\delta, \delta]$ have length at most $K\delta$.*

Proof. The discussion of "cookie-cutter sets" in [6] and in particular [6, Corollary 4.4] show that J is a *quasi-self-similar set.* More precisely, there exist $c > 0$ and $r_0 > 0$ such that for any $x_0 \in J$ and $r < r_0$ there exists a map $g : [x_0 - r, x_0 + r] \to \mathbb{R}$ with the properties

$$\begin{gathered} g(J \cap [x_0 - r, x_0 + r]) \subset J \\ cr^{-1}|x - y| \leq |g(x) - g(y)| \leq c^{-1}r^{-1}|x - y|\,, \quad x, y \in [x_0 - r, x_0 + r] \end{gathered} \tag{3.1}$$

Hence the proposition follows by a scaling argument. We remark that (3.1) also follows from the Koebe distortion lemma [3, Theorem 1.5]. □

Proof of Theorem 1. As outlined in the beginning of the section, we put $h = 1/|s|$, where $|\operatorname{Im} s|$ is large but $|\operatorname{Re} s|$ is uniformly bounded. We decompose the Julia set J into disjoint subsets:

$$I_j(h) := J \cap D_j + [-h, h]) = \bigcup_{p=1}^{P_j(h)} [x_p^j - r_p^j, x_p^j + r_p^j]\,, \quad x_{p+1}^j - r_{p+1}^j > x_p^j + r_p^j\,,$$

so that the intervals $[x_p^j - r_p^j, x_p^j + r_p^j]$ contain the connected components of $I_j(h)$. Proposition 3 shows that $r_p^j < Kh$ as $h \to 0$.

The open set $D(h)$ is defined as

$$D(h) = \bigcup_{j=1}^{2} D_j(h)\,, \quad D_j(h) = \bigcup_{p=1}^{P_j} D_{jp}(h)\,, \quad D_{jp}(h) = (x_p^j - r_p^j, x_p^j + r_p^j) + i(-h, h)\,,$$

and since $g_i : J \cap D_j^0 \to J \cap D_i^0$ we see that the condition (2.1) holds: for each D_{jp} there exists a $p' = p(i, j, p)$ for which

$$d(\partial D_{ip'}(h), g_i(D_{jp}(h))) > (1 - \beta)h\,,$$

for a fixed constant $0 < \beta < 1$. From this we also see that $P_j(h) = P(h)$ is independent of $j = 1, 2$.

It is classical that the Hausdorff measure of the Julia set is finite (see for instance [17] and the references given there) and hence $P(h) = \mathcal{O}(h^{-\delta})$.

We can now apply the same procedure as in the proof of Proposition 1. What we have gained is a bound on the weight: since $|\operatorname{Re} s| \leq C$ and g_i' is real on the real axis

$$|[g_i'(z)]^s| \leq C \exp(|s||\arg g_i'(z)|) \leq C \exp(C_1 |s||\operatorname{Im} z|) \leq C_2 \,, \quad z \in D_j(h) \,.$$

We write $\mathcal{L}(s)$ as a sum of four operators $\mathcal{L}_{ij}(s)$ each of which is a direct sum of $P(h)$ operators. The rectangles and the contracting prperties of g_i's are uniform after rescaling by h and hence the singular values of each of these operators satisfy the bound $\mu_l \leq C\gamma^l$, $0 < \gamma < 1$. Using (2.7) and (2.9) we obtain the bound

$$\log|\det(I - \mathcal{L}(s))| \leq CP(h) = \mathcal{O}(h^{-\delta}) \,,$$

and this is (1.6). □

Proof of Corollary 2. Proposition 2 shows that $Z(s)$ is given by (1.4) for $\operatorname{Re} s$ large. Hence for $\operatorname{Re} s > C_1$ we have $|Z(s)| > 1/2$. The Jensen formula then shows that the left hand side of (1.8) is bounded by

$$\sum \{ m(s) \; : \; |s - ir - C_1| \leq C_2 \} \leq 2 \max_{\substack{|s| \leq r + C_3 \\ |\operatorname{Re} s| \leq C_0}} \log|Z(s)| + C_4 \,,$$

and (1.8) follows from (1.6). □

4. Numerical evaluation of the zeta function

We have carried out an extensive set of numerical computations which suggest that the upper bound proved above is optimal. We have developed a fast algorithm for numerical evaluation of the zeta function, which we use for large-scale parallel computations of its zero pattern. The evaluation algorithm is based on the following convenient analytical setup. We have defined $\mathcal{L}(s)$ as an operator on holomorphic functions defined on an open neighbourhood D of the Julia set: in the analysis above we chose $D = D_1 \cup D_2$ with $D_j = (-1)^j(\sqrt{-\xi_c - c}, \xi_c)$ where $\xi_c = (1 + \sqrt{1-4c})/2$ is the largest fixed point of f_c. The Ruelle operator (1.2) is then given by (2.2). For numerical computations, we would like to choose another domain D to speed up the numerical evaluation of the determinant $Z(s) = \det(I - \mathcal{L}(s))$.

Assume $p = |c| > 4$. Then a first approximation to J is the union D^0 of two intervals

$$D_j = (-1)^j((p-\xi)^{\frac{1}{2}} - 1/4, \xi + 1/4) \,, \quad \xi = (1 + (1+4p)^{\frac{1}{2}})/2 \,.$$

Since

$$f(\pm\xi) = \xi \,, \quad f(\pm(p-\xi)^{\frac{1}{2}}) = -\xi \,,$$

the set of fixed points of iterates of f is contained in $D^0 = D_1 \bigcup D_2$. Moreover,

$$\overline{g_i(D_j)} \subset D_i \,, \quad \overline{g_j(D_1)} \cap \overline{g_j(D_2)} = \emptyset \,.$$

Thus this construction can be iterated. Let

$$D_{\underline{\mathrm{i}}} = g_{i_1} \circ \cdots \circ g_{i_{n-1}}(D_{i_n})$$

where the multiindex $\underline{\mathrm{i}}$ is defined by $\underline{\mathrm{i}} = (i_1, \cdots, i_n) \in \{1,2\}^n$. Then

$$D^n = \bigcup_{\underline{\mathrm{i}} \in \{1,2\}^n} D_{\underline{\mathrm{i}}}$$

approximates the Julia set accurately for large n. Since the g_j's are monotone, each $D_{\underline{\mathrm{i}}}$ is mapped into another by each g_j:

$$\overline{g_j(D_{\underline{\mathrm{i}}})} \subset D_{\sigma_j(\underline{\mathrm{i}})} \,, \quad \sigma_j(i_1, \cdots, i_n) = (j, i_1, \cdots, i_{n-1})$$

When p is large,

$$\xi = (1+(1+4p)^{\frac{1}{2}})/2 \simeq p^{\frac{1}{2}} + 1/2 + p^{-\frac{1}{2}}/8\,,$$
$$(p-\xi)^{\frac{1}{2}} \simeq p^{\frac{1}{2}} - 1/2 - p^{-\frac{1}{2}}/8\,.$$

On D^0 the derivatives of g_{ij}'s are approximately $p^{-1/2}/2$. Thus the sizes of the subintervals $D_{\underline{\mathrm{i}}}$'s are controlled by

$$|D_{\underline{\mathrm{i}}}| \simeq 2^{-n}p^{-n/2}\,, \quad \underline{\mathrm{i}} \in \{1,2\}^n\,.$$

The dimension should satisfy the following approximate relation

$$(\text{ size of the interval})^{-\delta} \simeq \text{number of intervals},$$

or

$$\delta \simeq \frac{2\log 2}{2\log 2 + \log p}$$

which agrees with rigorous estimates [10, 17].

4.1. **Determinant evaluation.** An efficient evaluation scheme chooses $D = D^n$ where n is large enough that

$$|D_{\underline{\mathrm{i}}}| \simeq |s|^{-1}\,, \quad \underline{\mathrm{i}} \in \{1,2\}^n$$

assuming that the intervals in the partition have roughly the same size $2^{-n}p^{-n/2}$. We expand each $D_{\underline{\mathrm{i}}}$ into a disc centered at the middle $a_{\underline{\mathrm{i}}}$ of $D_{\underline{\mathrm{i}}}$, and radius $r_{\underline{\mathrm{i}}}$ equal to half of the length of $D_{\underline{\mathrm{i}}}$. We denote the expanded discs also by $D_{\underline{\mathrm{i}}}$ for convenience. They can be computed in practice by mapping interval endpoints with the g functions and sorting the resulting intervals.

The transfer operator

$$\mathcal{L}(s)\ :\ \bigoplus_{\underline{\mathrm{i}}\in\{1,2\}^n} H^2(D_{\underline{\mathrm{i}}}) \longrightarrow \bigoplus_{\underline{\mathrm{i}}\in\{1,2\}^n} H^2(D_{\underline{\mathrm{i}}})$$

then becomes a sparse $2^n \times 2^n$ matrix of operators defined by

$$(\mathcal{L}(s))_{\underline{\mathrm{k}}\,\underline{\mathrm{m}}}\, u(z) = \begin{cases} [g_j'(z)]^s u(g_j(z))\,,\ u \in H^2(D_{\underline{\mathrm{m}}}) & \underline{\mathrm{m}} = \sigma_j(\underline{\mathrm{k}}) \\ 0 & \text{otherwise} \end{cases}$$

Numerically, we approximate $I - \mathcal{L}$ by a block matrix $I - L$ such as the ones shown in Figure 2.

Each matrix block approximates one operator $\mathcal{L}(s)_{\underline{\mathrm{k}}\,\underline{\mathrm{m}}}$ by a small matrix $L_{\underline{\mathrm{k}}\,\underline{\mathrm{m}}}$, which represents the compression of $\mathcal{L}(s)_{\underline{\mathrm{k}}\,\underline{\mathrm{m}}}$ onto the first $P+1$ elements of each orthonormal basis $\{\rho_p^{\underline{\mathrm{k}}}\}$ and $\{\rho_q^{\underline{\mathrm{m}}}\}$ for $H^2(D_{\underline{\mathrm{k}}})$ and $H^2(D_{\underline{\mathrm{m}}})$ respectively. Thus the matrix block $L_{\underline{\mathrm{k}}\,\underline{\mathrm{m}}}$ has elements

$$a_{pq} = \int_{D_{\underline{\mathrm{k}}}} \rho_p^{\underline{\mathrm{k}}}(z)[g_j'(z)]^s \rho_q^{\underline{\mathrm{m}}}(g_j(z))dz$$

where $\underline{\mathrm{m}} = \sigma_j(\underline{\mathrm{k}})$. [Note: it would probably be nice to add the formula for Z as the determinant of $I - PG^sH$.] This integral could perhaps be evaluated exactly, since only powers, logarithms and roots occur. However, exact formulas are likely to be cumbersome and expensive to evaluate, so we apply numerical integration techniques instead. The standard 21-point formula no. 25.4.61 on p. 892 of [2] is highly accurate, integrating up to tenth-degree polynomials exactly over a disc; adaptive quadrature could be used if even higher accuracy is desired. Once the block matrix L is computed, we evaluate the determinant $Z(s)$ by LU-factorization via standard LAPACK routines [1]. Efficiency is improved by careful precomputation and tabulation of common subexpressions. It could perhaps be improved further by sparse block QR decomposition as in [21], in view of the simple regular block structure evident in Figure 2.

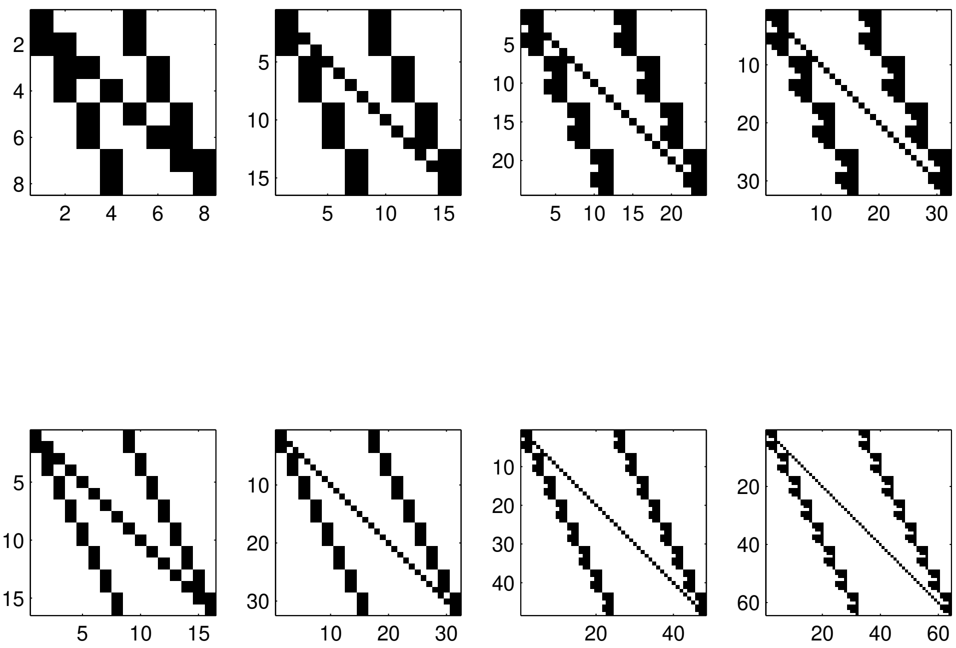

FIGURE 2. Block structure of matrix $I - L$ corresponding to Ruelle transfer operator for $N = 2^n = 8, 16$ (first and second rows) and $P = 1$, 2, 3 and 4 (left to right columns).

4.2. **Derivatives.** The zero-counting algorithm we describe below requires not only Z values, but also the values of the logarithmic derivative $Z'/Z = (\log Z)'$. Fortunately, these can easily be evaluated with the same apparatus used for Z itself. Indeed,

$$(\log\det(I - \mathcal{L}(s)))' = -\operatorname{tr}\left((I - \mathcal{L}(s))^{-1}\mathcal{L}'(s)\right)$$

so each block of the matrix L' involved in the evaluation of $Z'(s)$ has elements

$$b_{pq} = \int_{D_{\underline{k}}} \rho_p^{\underline{k}}(z)(\log[g_j'(z)])[g_j'(z)]^s \rho_q^{\underline{m}}(z)dz.$$

The matrix inverse $(I - \mathcal{L}(s))^{-1}$ is applied with the same LU-factorization (or QR-factorization) we used to evaluate the determinant, at essentially no additional expense. Thus the total cost of one evaluation of Z and its logarithmic derivative is $\mathcal{O}(N^3P^3)$ where $N = 2^n$ is the number of matrix blocks per dimension and P is the number of basis functions per disc. Usually we take n in the range 3 to 6 and P in the range 1 to 4, so the largest determinants and LU-factorizations we need to compute are about 256^2.

We verified the accuracy of the algorithm by an extensive series of refinement and comparison tests. For example, we computed the dimension δ for $c = -5$ with a succession of increasingly accurate parameter choices $n = 3, \ldots, 7$ and $P = 1, \ldots, 4$. The MATLAB zero-finding function FZERO with default tolerance 10^{-14} was used to compute the dimensions shown in Table 2. Since the exact value is 0.48479829443816, our evaluation scheme computes dimensions accurate to full double-precision accuracy with $n = 6$ and $P = 3$, by evaluating the determinants of 192×192 matrices. A preliminary implementation in the MATLAB rapid prototyping language [16] obtained

14-digit accuracy with $n = 6$ and $P = 3$ in 12.45 sec, running on one processor of a dual 1.8 GHz Xeon workstation running Red Hat Linux version 8 and MATLAB version 12. Three-digit accuracy required less than one second, but our prototype MATLAB implementation was still far too slow for the large-scale zero-counting which we report in Section 6 below. Thus the algorithm was rewritten in FORTRAN 77 and run on the UC Berkeley "Millennium" cluster containing about 250 Intel CPUs arranged in about 100 nodes.

TABLE 2. Dimension δ of the Julia set J for $c = -5$, computed with our evaluation scheme using n levels of intervals and P basis functions per disc.

	$P = 1$	2	3	4
$n = 3$	0.48478348721389	0.48479099537140	0.48479829294510	0.48479829372883
$n = 4$	0.48479741542081	0.48479784089445	0.48479829442433	0.48479829443523
$n = 5$	0.48479823885691	0.48479826617332	0.48479829443815	0.48479829443815
$n = 6$	0.48479829098609	0.48479829267778	0.48479829443816	0.48479829443816
$n = 7$	0.48479829422308	0.48479829432851	0.48479829443816	0.48479829443816

This should be compared to the numerical results of [10] where a different method of evaluating the zeta function was used. It follows the cycle expansion method based on rigorous results of Ruelle [19], and numerical investigations by Cvitanovič, Eckhardt and others [5]. Although the cycle expansion method has been used succesfully for computation of zeros (see [13] for a recent application), we found that our method allows larger values of $\mathrm{Im}\, s$ (see [9] for the use of the cycle expansion method following [10] in the context of Schottky groups).

Cycle expansions require careful grouping of large summands to detect the cancellations, which becomes increasingly difficult and unstable as the imaginary part of s increases; the summands grow exponentially.

5. Zero-counting algorithm

We apply a zero-counting algorithm to our FORTRAN implementation of $Z(s)$ to count the number of zeroes to the right of a line $\mathrm{Re}\, z = x$ between two horizontal lines $\mathrm{Im}\, z = s_0$ and $\mathrm{Im}\, z = s_1$. Since Z is holomorphic, the argument principle counts the number N of zeroes inside a closed curve Γ by the integral formula

$$N = \frac{1}{2\pi i} \int_\Gamma \frac{Z'(s)}{Z(s)} ds.$$

Numerical implementation of this formula turns out to be surprisingly tricky, because zeroes of Z induce poles of the integrand. (Figures 3 and 4 suggest how complicated and interesting the pole structure of Z'/Z can be.) Thus numerical integration over Γ with resolution h will work only if the zeroes of Z lie distance $\mathcal{O}(h)$ or more from Γ. Since the unknown zero locations may cluster anywhere, our choice of Γ must take Z values into account. Thus we have adopted the following zero-counting technique. First, we approximate only the integral over the vertical interval $\Gamma = [x + is_0, x + is_1]$ as the two horizontal lines contribute very little to the total. Next, we enclose the vertical interval V by zigzag contours Γ_L and Γ_R which give approximate upper and lower bounds $N_U \geq N_L$ for the number N of zeros; see Figures 3 and 4. Finally, we integrate the logarithmic derivative exactly over each segment of the contour.

Each zigzag contour is a polygonal line connecting a sequence of grid points $z_m = x + I_m h + i(s_0 + mh)$, where $h = 0.025$ is the half-width of the band enclosing Γ. The indices I_m are chosen

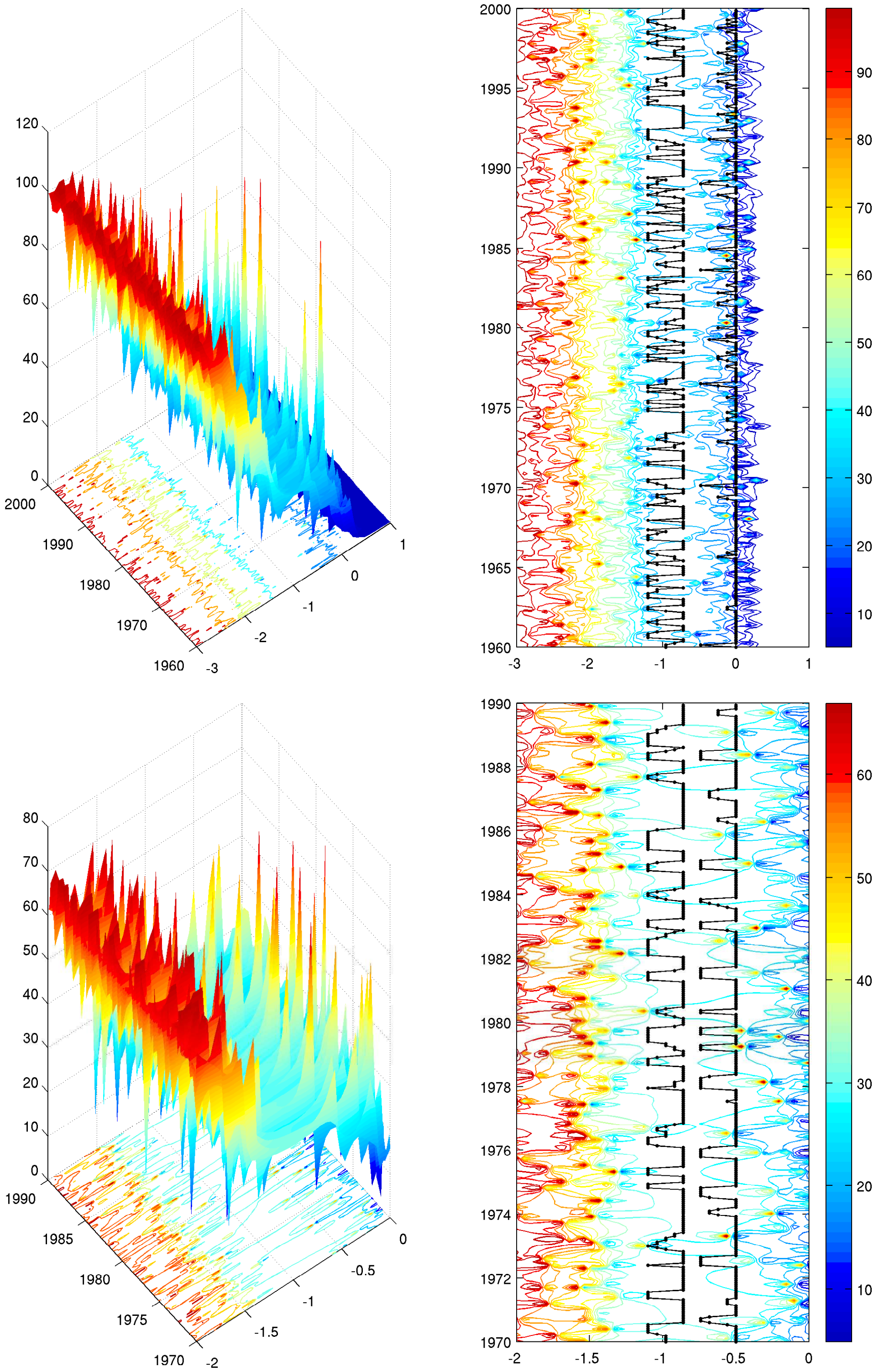

FIGURE 3. Surface and contours of $|Z'/Z|$ with $c = -10$, over the rectangle $-3 < \operatorname{Re} s < 1$, $1960 < \operatorname{Im} s < 2000$ and its central subrectangle $-2 < \operatorname{Re} s < 0$, $1970 < \operatorname{Im} s < 1990$. The zigzag contours shown in black steer to the right as much as possible, to avoid zeros and minimize the value of $|Z'/Z|$.

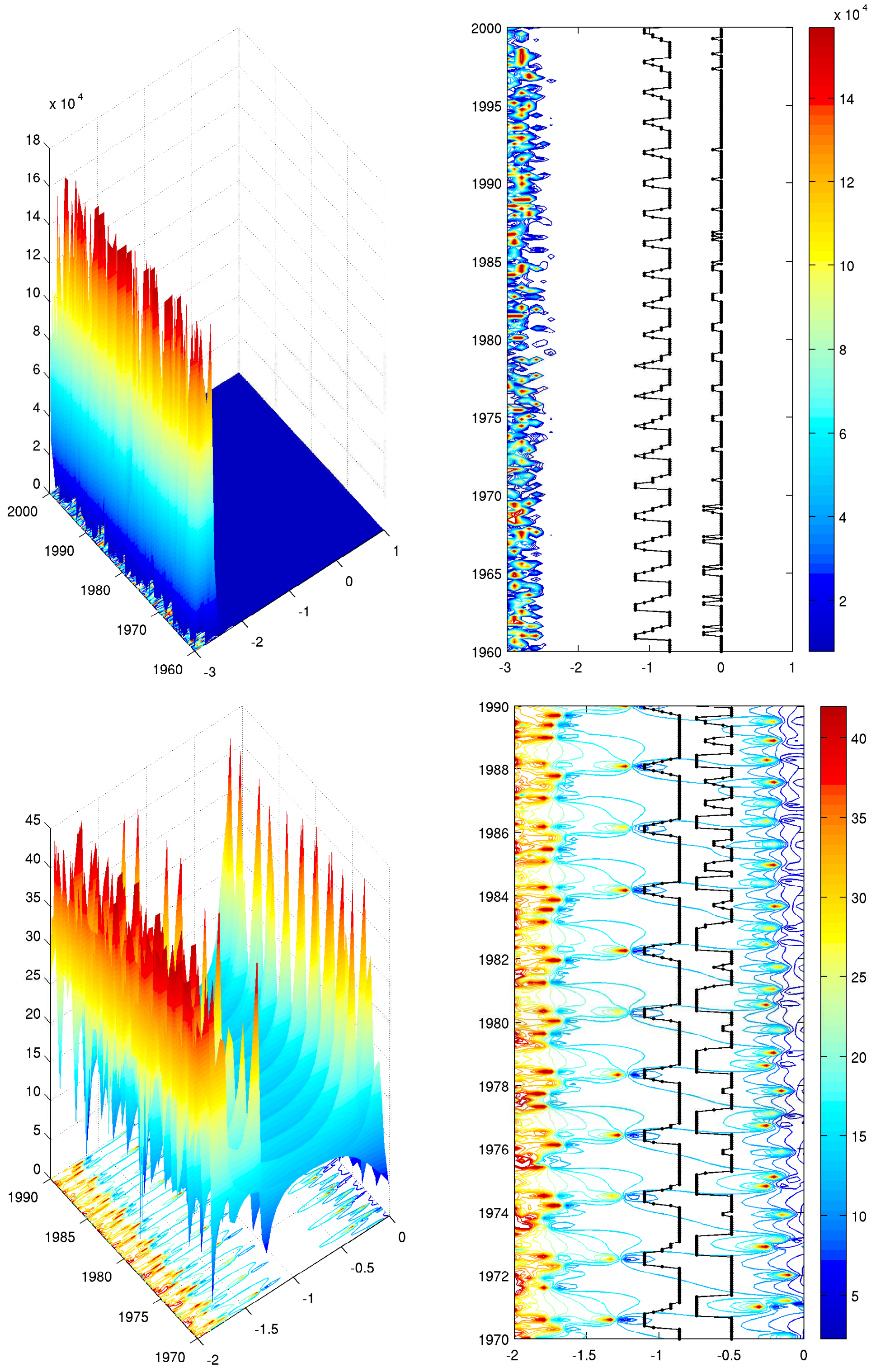

FIGURE 4. Surface and contours of $|Z'/Z|$ with $c = -160$, over the rectangle $-3 < \operatorname{Re} s < 1$, $1960 < \operatorname{Im} s < 2000$ and its central subrectangle $-2 < \operatorname{Re} s < 0$, $1970 < \operatorname{Im} s < 1990$.

between $-Q$ and Q inclusive (usually $Q = 5$ or so) to minimize the integrand:

$$\frac{|Z'(z_m)|}{|Z(z_m)|} = \min_{|q|\leq Q} \frac{|Z'(x+qh+i(s_0+mh)|}{|Z(x+qh+i(s_0+mh))|}.$$

Integrating over this contour gives exactly

$$N_J = \frac{1}{2\pi i}\int_{\Gamma_J} \frac{Z'(s)}{Z(s)} ds = \frac{1}{2\pi i}\sum_{m=1}^{M-1} \log\left(\frac{Z(z_{m+1})}{Z(z_m)}\right)$$

for $J = U, L$.

6. Numerical conclusions

We used the above algorithm to compute the density of zeros of the zeta function $Z(s)$ for many values of the parameter $c < -2$. The numerical results strongly support Conjecture 3 stated after Corollary 2 in Section 1. We stress that our computations are *empirical*, that is we cannot prove the convergence rigorously – we only see convergence when the parameters which improve accuracy increase. The upper bounds techniques of Section 2 give estimates guaranteeing convergence but they are numerically feasible for small values of $|\operatorname{Im} s|$ only: the size of L and P required grows too fast.

The zero counting algorithm presented in Section 5 gives us upper and lower bounds for the number of zeros, $n(r,x)$ with $\operatorname{Re} s > -x$ and $0 \leq |\operatorname{Im} s| \leq r$:

$$n_L(r,x) \leq n(r,x) \leq n_U(r,x)\,.$$

As seen in Figures 3 and 4 the density of zeros is large and the distribution too irregular to obtain a completely accurate evaluation of $n(r,x)$ when r large. The upper bound given in Corollary 2 is the same as

$$\log n_U(r,x) \leq (1+\delta)\log r + B_U(x)\,,$$

and ideally we would like to have

$$\log n_L(r,x) \geq (1+\delta)\log r + B_L(x)\,, \quad x > x_0(c)\,. \tag{6.1}$$

For a given c we calculate $n_\bullet(r,x)$ for $r \leq R$ using parameters L, P suggested by the proof of the upper bound, that is ones for which the behaviour of the transfer operator is nicely controlled for $\operatorname{Im} s \sim R$. That means that we require $2^L \sim |\operatorname{Im} s|^\delta$, and we take $P = 1$ or 2. As explained in Section 4.1 the increase of L is very costly and we use larger values of the parameters only to test the accuracy of our results. The plots of $\log n_\bullet(r,x)$ against $\log r$ for different values of x are shown on the left of Figure 5.

To see if (6.1) has a chance of being true we use the least squares method to approximate $\log n_\bullet$ as a function of $\log r$:

$$n_\bullet(r,x) \simeq A_\bullet(x)\log r + B_\bullet(x)\,, \quad r \leq R\,, \tag{6.2}$$

where $\bullet = L, U$ corresponds to the upper and lower bounds respectively. Although $n_L(r,x) \leq n_U(r,x)$ it may happen that $A_L(x) > A_U(x)$ due to the irregularities in distributions.

The lower bound (6.1) can be loosely reformulated as

$$A_L(x) \simeq A_U(x) \simeq 1 + \delta\,, \quad x \geq x_0\,.$$

That this happens for $c = -10$ and $c = -100$ is shown in on the right of Figure 5

These results are typical for what we obtained for other values of c. Although for larger $|c|$'s we can use a lower L to reach higher values of $\operatorname{Im} s$ accurately, we observe a phenomenon of "conservation of difficulty". That is seen in the comparison between Figures 5 (a) and (b): convergence to the dimension for $c = -160$ requires $\operatorname{Im} s$ ten times as large as for $c = -10$.

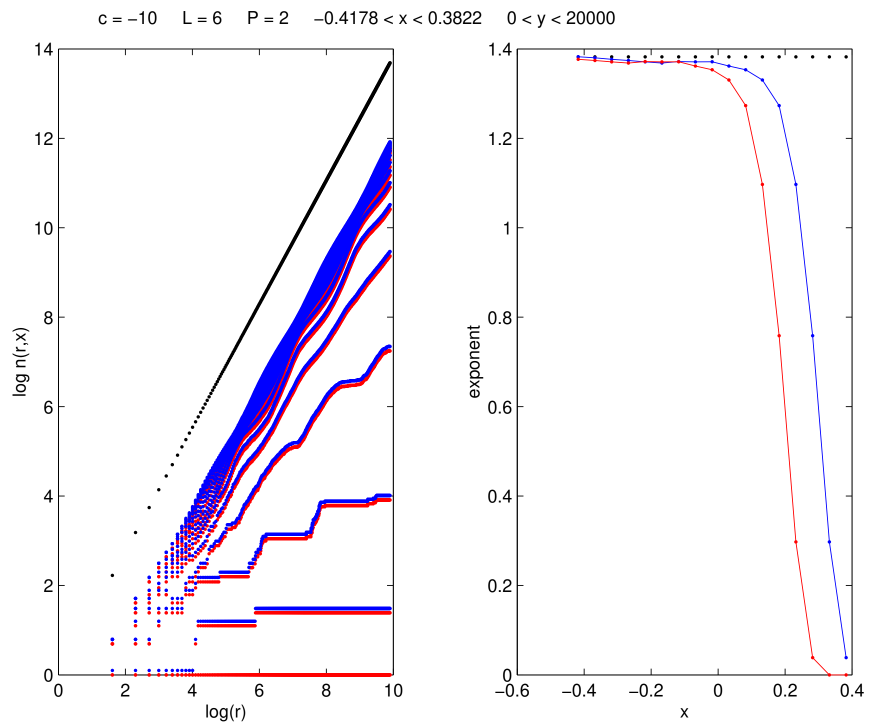

(a)

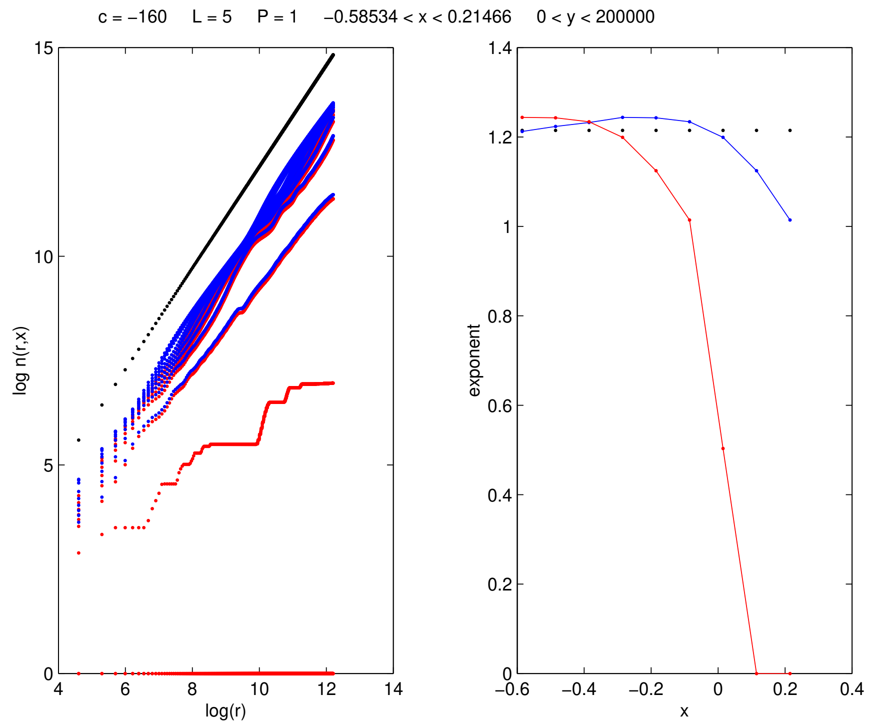

(b)

FIGURE 5. Number of zeroes $n(r, x)$ vs. $\log r$ and corresponding exponents $1+\delta$. (a) $c = -10$, $L = 6$,$P = 2$, $0 \le r \le 20000$, $0.3822 > x > -0.4178$ in 17 steps of 0.05. (b) $c = -160$, $L = 5$, P = 1,$0 \le r \le 200000$, $0.58534 > x > -0.28534$ in 9 steps of 0.1.

7. Open questions suggested by numerical data

The code we produced offers possibilities for future research. Two directions are suggested by recent developments. Naud's [15] adaptation of Dolgopyat's method to this setting of Schottky quotients and Julia sets shows that there exists a constant $\epsilon = \epsilon(c)$ such that $Z(s)$ is zero-free for s in the strip $\delta(c) - \epsilon(c) < \operatorname{Re} s < \delta(c)$. In this paper, we have not attempted to analyze ϵ as a function of c, though some dependence is apparent in the figures.

Another direction is suggested by [13], where it was pointed out that zeros are denser near a particular value $\operatorname{Re} s$ related to the classical escape rate. We have seen such a concentration of zeros in Figures 3 and 4, but we have not computed the classical escape rate for comparison.

References

[1] E. Anderson et al., *LAPACK Users' Guide*, SIAM, Philadelphia, 1992.
[2] M. Abramowitz and I. A. Stegun, *Handbook of Mathematical Functions*, Dover, 1965.
[3] L. Carleson and T.W. Gamelin, *Complex Dynamics*, Springer Verlag, 1993.
[4] H. Christiansen, *Growth and zeros of the dynamical zeta function for hyperbolic rational maps,* preprint, 2003.
[5] B. Eckhardt, G. Russberg, P. Cvitanović, P. E. Rosenqvist, P. Scherer, "Pinball Scattering," in *Quantum Chaos*, Cambridge Univ. Press 1995, 405-433.
[6] K. Falconer, *Techniques in fractal geometry,* J. Wiley & Sons, 1997.
[7] D. Fried, *The Zeta functions of Ruelle and Selberg,* Ann. Sc. Éc. Norm. Sup, **19**(1986), 491-517.
[8] I.C. Gohberg and M.G. Krein, *An introduction to the theory of linear non-self-adjoint operators,* Translation of Mathematical Monographs, **18**, A.M.S. Providence, 1969.
[9] L. Guillopé, K. Lin, and M. Zworski, *The Selberg zeta function of convex co-compact Schottky groups.* to appear in Comm. Math. Phys.
[10] O. Jenkinson and M. Pollicott, *Calculating Hausdorff dimension of Julia sets and Kleinian limit sets,* Amer. J. Math. **124**(2002), 495-545.
[11] K. Lin, *Numerical study of quantum resonances in chaotic scattering*, J. Comp. Phys. **176**(2002), 295-329.
[12] K. Lin and M. Zworski, *Quantum resonances in chaotic scattering*, Chem. Phys. Lett. **355**(2002), 201-205.
[13] W. Lu, S. Sridhar, and M. Zworski, *Fractal Weyl laws for chaotic open systems,* `nlin.CD/0208019`, to appear in Phys. Rev. Lett.
[14] M. Lyubich and Y. Minsky, *Laminations in holomorphic dynamics,* J. Diff. Geom. **47**(1997), 17-94.
[15] F. Naud, *Expanding maps on Cantor sets, analytic continuation of zeta functions with applications to convex co-compact surfaces*, preprint, 2003.
[16] The MathWorks Inc., *MATLAB Reference Guide*, The MathWorks Inc., 1992.
[17] C. McMullen, *Hausdorff dimension and conformal dynamics III: Computation of dimension*, Amer. J. Math. **120**(1998) 691–721.
[18] S.J. Patterson and P. Perry, *Divisor of the Selberg zeta function for Kleinian groups in even dimensions, with an appendix by* C. Epstein, Duke. Math. J. **326**(2001), 321-390.
[19] D. Ruelle, *Zeta-functions for expanding Anosov maps and flows,* Inv. Math. **34**(1976), 231-242.
[20] J. Sjöstrand, *Geometric bounds on the density of resonances for semiclassical problems*, Duke Math. J. **60**(1990), 1-57.
[21] J. Strain, *Fast stable deferred correction methods for two-point boundary value problems,* preprint 2003.
[22] M. Zworski, *Dimension of the limit set and the distribution of resonances for convex co-compact hyperbolic surfaces,* Inv. Math. **136**(1999), 353-409.
[23] M. Zworski, *Resonances in Physics and Geometry,* Notices Amer. Math. Soc. **46**(1999), 319-328.

Mathematics Department, University of California, Evans Hall, Berkeley, CA 94720, USA
E-mail address: `strain@math.berkeley.edu`
E-mail address: `zworski@math.berkeley.edu`